

ABSOLUTE PHOTOMETRY OF THE SOUTHERN ORION REGION IN THE VACUUM ULTRAVIOLET (1300-2000 Å)

WATARU TANAKA, TAKASHI ONAKA, AND MINEO SAWAMURA
Department of Astronomy, University of Tokyo

AND

TETSUYA WATANABE, KEIICHI KODAIRA, AND KEIZO NISHI
Tokyo Astronomical Observatory

Received 1983 April 7; accepted 1983 October 24

ABSTRACT

Absolute photometry of the southern Orion region was carried out for five passbands in the vacuum ultraviolet (1300-2000 Å, $\Delta\lambda = 84$ Å) with a rocket-borne spectrometer. More than 60 early-type stars and the diffuse background radiation were observed within the raster-scanned field of $8^\circ \times 8^\circ$ centered at $\alpha = 5^{\text{h}}30^{\text{m}}$ and $\delta = -4^\circ$. Stellar data suggest a revision of the current absolute scale by 10%-30%, which relatively suppresses the flux toward shorter wavelengths. The present data of the background radiation have the highest spectral resolution among those published and indicate a steep systematic increase of the flux toward shorter wavelengths. Direct consequences of the new calibration are briefly discussed.

Subject headings: photometry — stars: early-type — ultraviolet: general

I. INTRODUCTION

An ultraviolet spectrometer attached to a 30 cm reflector was loaded at the top of an attitude-controlled S520-type sounding rocket provided by the Institute of Space and Astronautical Science (ISAS)/Japan and launched at 10:50 UT (= 19:50 JST) on 1982 February 14 from the Kagoshima Space Center/ISAS. The rocket reached a maximum altitude of 266 km at $T = 261$ s after the launch and raster-scanned three times over an $8^\circ \times 8^\circ$ field with $16'$ FOV in the southern Orion region centered at $\alpha = 5^{\text{h}}30^{\text{m}}$ and $\delta = -4^\circ$ (1950.0), from $T = 100$ -400 s (altitude > 150 km). The purpose of this experiment was twofold: the absolute calibration of stellar fluxes and the measurement of the diffuse background radiation in the wavelength range 1300-2000 Å.

Independent absolute calibrations were carried out for OAO 2 (Code and Meade 1979), TD-1 (Jamar *et al.* 1976; Macau-Hercot *et al.* 1978), and ANS (Wesselius *et al.* 1980), but the calibration by the rocket experiment of the Johns Hopkins University group (Brune, Mount, and Feldman 1979) was transferred to IUE through observations of a few stars in common (Bohlin *et al.* 1980). Intercomparisons among them and those of other sources (Stecher 1968; Henry *et al.* 1975; Strongylis and Bohlin 1979) revealed that residual uncertainties may still amount to up to 10% for 1400-2000 Å and to more than that for $\lambda < 1400$ Å (cf. Bohlin *et al.* 1980). Rockets are known to be superior to satellites for the purpose of the absolute calibration because of the shorter preparation period, but inferior because of the extremely limited observation time which in turn usually limits the number of program stars to a few or so. The present experiment yielded data for more than 60 Orion stars by raster-scanning, though the signal-to-noise ratios for individual stars were relatively low, and enabled us to derive mean relations between our absolute scale and those for different satellites, less affected by peculiar properties of individual stars, if any. The raster-scanning observation

provided us also with the data of diffuse background radiation in the Orion region in the absolute scale. In this paper we present a new absolute calibration and point out its direct consequences. The detailed studies of stellar fluxes and of the background radiation will be published separately.

II. INSTRUMENTATION AND CALIBRATION

The optical layout of the telescope and spectrometer system is shown in Figure 1. The primary mirror of the F/5.9 modified Cassegrain system had an aperture of 292 mm with an off-axis oval center bore (100 mm \times 150 mm) to accommodate the spectrometer. The primary and the secondary mirrors were aluminized and coated with MgF_2 . Deep sky baffles with stray-light stoppers were provided around the secondary and the entrance diaphragm of the spectrometer, inhibiting direct views of both elements from outside. The spectrometer had a circular entrance diaphragm corresponding to $16'$ on the sky, and as a disperser a holographic concave grating (1860 gr mm^{-1} , 100 mm \times 100 mm, F/5) produced by Jobin Yvon/France. Five Cs-Te cathode photomultipliers of 13 mm diameter (HTV R1080) were set up each in a separation of 15 mm along the Rowland circle of the concave grating and provided with a mask of 8 mm \times 8 mm opening which determined the bandpass of ± 42 Å. The central wavelengths of the five bands are given in Table 1. The main scanning direction of the rocket along the line of right ascension was set equal to the direction of the dispersion of the spectrometer, allowing a spectral scan over an additional range of ± 42 Å when a stellar image crossed over the full diameter of the diaphragm. Five independent photon-counting systems were employed with 16 bit binary counters. Count rates in every 5 ms were transmitted to the ground with a multichannel PCM telemeter.

The calibrations were done at the Vacuum Ultraviolet Laboratory of the Tokyo Astronomical Observatory (cf. Nishi and Suemoto 1971). The spectral reflectivities of the telescope

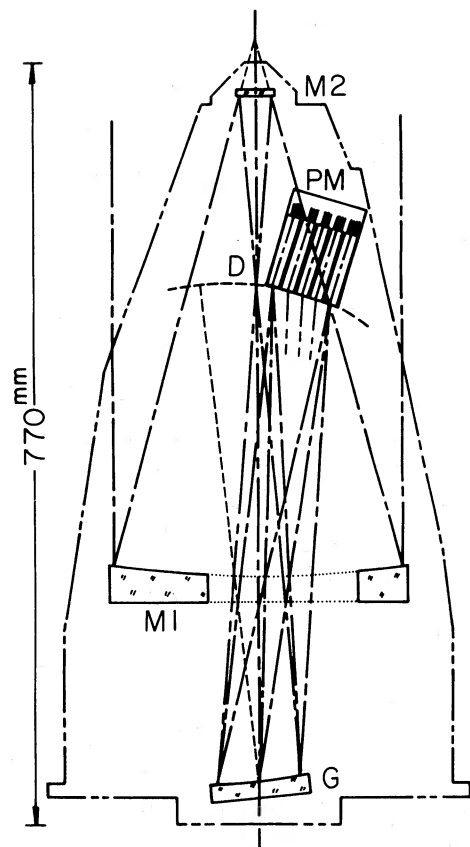


FIG. 1.—Optical layout of the telescope and spectrometer system. M1: primary mirror; M2: secondary mirror; D: diaphragm; G: concave grating; and PM: photomultiplier package. The outline of the whole instrument is also indicated.

mirrors were determined by measuring five test pieces which were aluminized and coated together with the primary and the secondary. In the plating chamber, three test pieces were laid separately by 120° around the primary and one in the center bore. No difference was found among the reflectivities of the four. The other one was laid next to the secondary. In the actual reflectivity measurement, the light beam (4 mm diameter) from a monochromatic collimator was led to the test piece set in a movable holder with an incident angle of 6 degrees. The intensities of the reflected beam were compared

with those of the incident beam using a photomultiplier with a sodium salicylate coated window, which was mounted on a rotatable arm to facilitate the measurement. Temporal variations of reflectivity were monitored using the test pieces before and after the launch of the rocket, proving to be negligible. The spectral efficiency of the grating was measured with the same equipment by the same principle as above. Systematic changes due to the minor differences in the setting of the grating and the detector between the laboratory and the flight have been proved to be negligible by virtue of the small incident angle (cf. Nishi, Higashi, and Yamaguchi 1970; Hunter 1974). The blazing wavelength of the grating was set to be 1500 \AA ; however, the efficiency curves of both positive and negative first orders were nearly the same and flat around 20%. The quantum efficiencies of the photomultipliers operated in the photon-counting mode were determined by referring to the photodiode (EMR Schlumberger Model 543P-09-00) which had been absolutely calibrated at the National Bureau of Standards/USA. The measurements were done by using the same electronic circuits as the flight model. At first the pulse height characteristics were analyzed for determining the discrimination levels. Then the linearities were checked by a comparison with a calibrated photomultiplier (EMR Model 542G-09-18) and by varying the slit size of the light source. The direct comparison of the photon-counting detector system with the calibrated photodiode was difficult because of the large difference in their sensitivities. A photomultiplier (HTV 6199) with a sodium salicylate coated window was used to interrelate these detectors by virtue of its large dynamic range. It had been proved that sodium salicylate had suitable characteristics both in spectral response and in linearity. The positional variations of quantum efficiencies were carefully measured over the cathode surfaces of the photomultipliers and taken into account in deriving stellar fluxes. After determining the trajectories of stellar images across the diaphragm from the raster-scanning path (see below) and the response time profile, we integrated the quantum efficiencies along the strips of spectral images on the cathode surfaces, to obtain effective efficiencies for individual observations. The detection limit of the whole system was found to be about $10^{-11} \text{ ergs cm}^{-2} \text{ s}^{-1} \text{ \AA}^{-1}$ at 1500 \AA ($0.8 \text{ photons cm}^{-2} \text{ s}^{-1} \text{ \AA}^{-1}$, $m_{1500} = 6.3$) for the adopted spatial raster-scanning rate of 2° s^{-1} . The laboratory data are summarized in Table 1. Since the rocket instrument was not recovered, we have no positive guarantee for the assumed constant instrumental performance throughout the pre- and in-flight period. The highest danger may have been

TABLE 1
SENSITIVITY CALIBRATION DATA

Central Wavelength λ_c (Å)	Reflectivity of Primary $R_p(\lambda_c)$	Reflectivity of Secondary $R_s(\lambda_c)$	Efficiency of Grating $R_g(\lambda_c)$	Quantum Efficiency of Photomultiplier $E(\lambda_c)^a$	Effective Area $A(\lambda_c)^b$ (cm ²)
1328.....	0.71	0.66	0.184	0.037	1.5
1484.....	0.70	0.63	0.204	0.053	2.2
1640.....	0.66	0.61	0.189	0.089	3.1
1796.....	0.69	0.61	0.183	0.122	4.3
1951.....	0.75	0.67	0.183	0.123	5.2

^a At the center of the cathode.

^b $A(\lambda_c) = S \times R_p(\lambda_c) \times R_s(\lambda_c) \times R_g(\lambda_c) \times E(\lambda_c)$, where S is the unvignetted area of the primary 459 cm^2 .

the possible contamination of the primary and secondary mirrors by gases evaporating from the inner surface of the rocket nose cone if this had been strongly heated up during the initial upleg period. According to the experimental data provided by ISAS, the temperature of the inner surface of the nose cone made of FRP (fiber reinforced plastics) reaches the maximum between 70° C and 130° C shortly before it is opened up. We assume that the contamination was negligible.

III. DATA ANALYSIS AND DISCUSSION

The raster-scanned path of the rocket was determined by iteration using the read-outs of the attitude-controlling gyroscopes and the identified stellar positions. During the three frames of the raster-scanning, the telescope field of view covered all stars with flux more than 10^{-9} ergs cm^{-2} s^{-1} \AA^{-1} at 1951 \AA in the $8^\circ \times 8^\circ$ target area, with only one exception of σ Ori. About 200 discrete source detections were recorded in total, and the integrated photon counts in 1951 \AA channel exceeded 75 over the background level for 149 of these, the maximum being 73,620 counts for δ Ori. Of these detections, 138 were identified as being 62 early-type stars; thus, each star was measured twice on average, and seven objects were observed more than twice. A correlation analysis between the stellar signals and the background indicates that the effects of stray light are negligible in the following analysis. The dark-noise levels of the detector systems were less than 1 count s^{-1} .

The mean ratios of the absolute fluxes observed by us to those of *OA O 2* (Code and Meade 1979) are plotted in Figure 2. Fluxes of 26 stars commonly observed by us and *TD-1* (Jamar *et al.* 1976; Macau-Hercot *et al.* 1978) are compared and transformed into the *OA O 2* scale using Beekmans' (1977) calibration. For the band of the shortest wavelength (1328 \AA), we have only six stars available for the direct comparison with *OA O 2*. The accuracy of the mean ratio for this 1328 \AA band

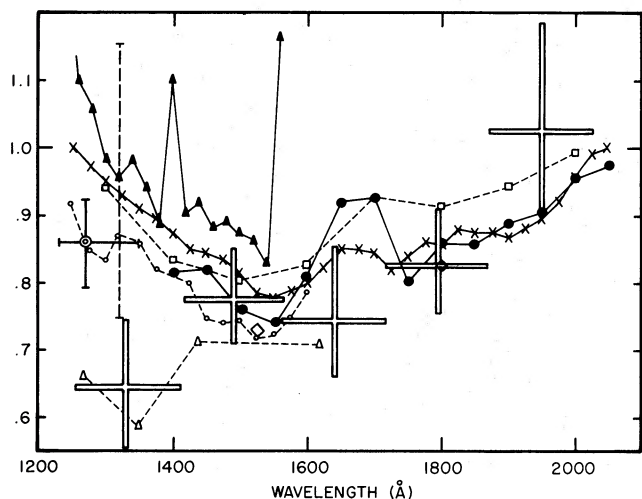


FIG. 2.—Flux ratio to *OA O 2* scale (S520-3; bars). For comparison, the ratios of *TD-1* (filled circles), *ANS* (rhombi), and *IUE* (crosses) to *OA O 2* are also plotted according to Beekmans (1977), Wesselius *et al.* (1980), and Bohlin *et al.* (1980), respectively. Calibration using η UMa by Apollo 17 (Henry *et al.* 1975; open circles) and rockets (Stecher 1968; squares; Opal *et al.* 1968; open triangles) are plotted according to Bohlin *et al.* (1980). Observations of the Orion region by Carruthers (1969) and Carruthers *et al.* (1981) are plotted with double circles and filled triangles (error ranges are also indicated).

was examined by applying the same six stars also to all other four passbands. Within 5% accuracy, the mean ratios obtained from the direct comparison of the six stars were found to be consistent to those obtained from the comparison of the 26 common stars to *TD-1* when transformed using *TD-1* versus *OA O 2* correction. Therefore, the result of the shortest wavelength band is supposed not to be strongly biased by the selection effects. The error bars of the present data include the uncertainties in the instrumental calibrations, the uncertainties in the path determinations, and the dispersion (1σ) in deriving the average values for sample stars. For the purpose of a detailed comparison, the flux data of the 62 identified stars are given in Table 2, together with those observed by *TD-1* and *OA O 2* whenever available.

The new calibration suggests that (1) revisions of about +10% and -10% are due around 2000 \AA and 1640 \AA , respectively, and that (2) a correction of about -30% is necessary around 1300 \AA . These corrections as a whole suppress the flux below 1500 \AA relative to that above 1800 \AA . Figure 3 shows the flux distribution of ν Ori, a B0 V star observed by *OA O 2*, *TD-1*, *ANS*, Carruthers (1969), and by us. Our data seem to be smoothly connected to the ion-chamber observation of Carruthers (1969). As shown in Figure 4, we can compare the observation with the model prediction of Kurucz (1979), though the effects of the effective temperature and the interstellar absorption are nearly equivalent in these wavelengths (Carruthers, Heckathorn, and Opal 1981). If we adopt the model atmosphere with the effective temperature 30,000 K ($\log g = 4.0$), which is the nearest to the effective temperature of B0 V star in the scale of Böhm-Vitense (1981), a reddening of $E(B-V) = 0.04-0.08$ is required for the fitting of our observation, assuming the extinction curve of Savage and Mathis (1979). This value of $E(B-V)$ is somewhat larger than that deduced from observations of ν Ori in the optical region, $E(B-V) = 0.02-0.04$ (Blanco *et al.* 1968; FitzGerald 1970; see Jamar *et al.* 1976). There might be uncertainties of this amount in the photometric observation of marginally reddened stars. Another possibility is that the interstellar matter toward ν Ori may have a higher extinction efficiency in the vacuum ultraviolet region than the average curve indicates (cf. Meyer and Savage 1981). In case no interstellar extinction is considered, our flux distribution falls at best between the model curves for 20,000 K and 22,500 K, the best fit model to the *IUE* data being 25,000 K.

The new calibration is also applied to the flux distribution of A type stars. Previously Kurucz (1979) found his model atmosphere of $T_{\text{eff}} = 9,400$ K ($\log g = 3.95$) to fit with the observations of α Lyr, while Dreiling and Bell (1980) determined the effective temperature of α Lyr as $T_{\text{eff}} = 9,650 \pm 200$ K ($\log g = 3.75 \pm 0.25$) based upon various observations including line spectra. The latter found that the fluxes between 1200 and 3300 \AA of the 9650 K model generally agree with the *OA O 2* observations of α Lyr when transformed into the *IUE* scale after Bohlin *et al.* (1980). Figure 5 shows the flux distribution of α Lyr after our correction factors are used to recalibrate *OA O 2* data. We applied a constant correction factor to the wavelength points within each passband of our system. Corrected UV fluxes shows an improved fitting with a model of $T_{\text{eff}} = 9,400$ K ($\log g = 3.95$), when the geometrical dilution factor $(d/R)^2 = 1.62 \times 10^{16}$ is adopted after Dreiling and Bell (1980).

TABLE 2
FLUX DATA OF THE 62 STARS OBSERVED BY THE S520-3 EXPERIMENT

HDNo. Sp.	FLUX(erg/cm sec A) ²			HDNo. Sp.	FLUX(erg/cm sec A) ²					
	1328A	1484A	1640A		1796A	1640A	1796A	1951A		
33928 B8-5 V	8.44E-11	7.17E-11	5.24E-11	5.01E-11	6.05E-11	36916 B9	5.78E-11	5.49E-11	4.83E-11	4.19E-11
34503 B5 III	6.81E-10	1.04E-09	5.45E-10	7.19E-10	9.23E-10	36960 B0 V	2.40E-09	1.37E-09	1.42E-09	1.20E-09
(TD-1)		9.93E-10	8.63E-10	6.39E-10	6.14E-10	(TD-1)	2.65E-09	2.08E-09	1.63E-09	1.22E-09
34511 B5 V	7.11E-11	7.37E-11	4.24E-11	3.47E-11	2.80E-11	37018 B2 III	2.18E-09	1.21E-09	1.23E-09	9.85E-10
34835 B8	5.25E-11	3.43E-11	1.91E-11	1.57E-11	1.40E-11	(TD-1)	1.98E-09	1.67E-09	2.07E-09	1.91E-09
34880 B9	7.51E-11	7.03E-11	2.83E-11	3.94E-11	4.00E-11	37041*O9.5 V	4.95E-09	2.58E-09	2.67E-09	2.56E-09
35008 B8	3.95E-11	3.95E-11	2.41E-11	2.66E-11	2.36E-11	37043 O9 III	1.09E-08	6.32E-09	7.00E-09	7.35E-09
35039 B2 IV	1.12E-09	7.80E-09	7.80E-10	7.81E-10	7.65E-10	(TD-1)	9.62E-09	7.54E-09	6.62E-09	5.61E-09
35079 B8	1.14E-09	6.83E-11	3.98E-11	4.07E-11	3.13E-11	(OAO-2)	1.36E-08	9.13E-09	8.43E-09	6.16E-09
35239 B2 V	6.81E-10	5.20E-10	3.53E-10	2.90E-10	3.20E-10	37055 B3 V	1.78E-10	9.26E-11	8.36E-11	9.87E-11
(TD-1)		5.54E-10	4.99E-10	3.53E-10	2.68E-10	(TD-1)	1.40E-10	1.17E-10	9.12E-11	7.47E-11
35411 B1 V	4.08E-09	4.82E-09	2.93E-09	3.12E-09	2.58E-09	37128 B0 Ia	1.91E-08	9.89E-09	1.14E-08	1.26E-08
(TD-1)		4.53E-09	3.54E-09	2.84E-09	2.07E-09	(TD-1)	1.65E-08	1.28E-08	1.20E-08	1.01E-08
(OAO-2)		6.02E-09	4.15E-09	3.45E-09	2.35E-09	(OAO-2)	2.95E-08	1.46E-08	6.17E-11	6.78E-11
35502 B5 V	5.95E-11	6.99E-11	3.34E-11	2.95E-11	2.97E-11	37129 B2 Vp	1.14E-10	6.84E-11	5.68E-11	4.69E-11
35548 B9	3.50E-11	1.12E-11	1.26E-11	2.84E-11	2.39E-11	(TD-1)	9.05E-11	6.90E-11	2.20E-10	2.00E-10
35575 B3 V	2.31E-10	1.87E-10	1.35E-10	1.22E-10	1.24E-10	37150 B3 V	4.42E-10	2.93E-10	2.20E-10	2.00E-10
(TD-1)		1.70E-10	1.40E-10	1.11E-10	8.44E-11	37151 B8 V	5.42E-11	2.39E-11	1.98E-11	2.18E-11
35640 B9 V	6.34E-11	4.99E-11	4.74E-11	3.51E-11	3.26E-11	37209 B1 V	6.07E-10	3.72E-10	3.38E-10	3.54E-10
35777 B2 V	2.05E-10	1.48E-10	9.57E-11	9.57E-11	7.64E-11	(TD-1)	6.20E-10	4.93E-10	2.76E-10	2.89E-10
(TD-1)		1.53E-10	1.25E-10	9.95E-11	7.70E-11	37303 B1 V	4.75E-10	3.23E-10	2.76E-10	2.60E-10
35971 B9	3.30E-11	3.53E-11	2.55E-11	2.74E-11	2.93E-11	(TD-1)	4.48E-10	3.49E-10	2.81E-10	2.10E-10
36046 B9	3.58E-11	4.00E-11	1.49E-11	1.67E-11	1.97E-11	37321 B3 V	1.34E-10	5.69E-11	5.06E-11	4.45E-11
36058 B9	5.29E-11	3.31E-11	2.27E-11	2.27E-11	2.19E-11	37332 B8	8.92E-11	4.62E-11	3.26E-11	3.13E-11
36151 B5 V	1.56E-10	1.00E-10	6.46E-11	6.11E-11	6.32E-11	37334 B3	1.43E-10	1.12E-10	7.96E-11	7.24E-11
36219 B9	3.75E-11	3.86E-11	2.14E-11	1.50E-11	1.31E-11	37356 B1.5 V	2.88E-10	1.50E-10	1.26E-10	1.08E-10
36285 B1.5 V	4.04E-10	3.09E-10	2.07E-10	1.58E-10	1.55E-10	37397 B3 V	1.97E-10	8.79E-11	7.88E-11	6.18E-11
(TD-1)		2.54E-10	2.03E-10	1.74E-10	1.33E-10	(TD-1)	1.12E-10	9.06E-11	7.17E-11	5.81E-11
36430 B2 V	3.61E-10	2.23E-10	1.74E-10	1.61E-10	1.19E-10	37481 B1 V	6.34E-10	2.73E-10	3.03E-10	2.43E-10
(TD-1)		2.38E-10	1.96E-10	1.53E-10	1.21E-10	(TD-1)	4.75E-10	2.31E-10	3.07E-10	2.30E-10
36486 O9.5 II	1.77E-08	1.40E-08	1.04E-08	9.13E-09	9.85E-09	37507 A4 IV	4.56E-10	3.31E-10	2.47E-11	3.65E-11
(TD-1)		1.41E-08	1.00E-08	9.86E-09	8.55E-09	(TD-1)	1.05E-11	1.05E-11	2.72E-11	2.97E-11
(OAO-2)		1.76E-08	1.11E-08	9.48E-09	9.48E-09	37526 B3 V	5.40E-11	2.23E-11	2.52E-11	2.82E-11
36512 B0 V	3.03E-09	2.55E-09	1.45E-09	1.33E-09	1.22E-09	37642 B9	4.06E-11	2.57E-11	1.76E-11	1.69E-11
(TD-1)		2.56E-09	1.90E-09	1.52E-09	1.23E-09	37687 B8	2.93E-11	2.22E-11	2.64E-11	2.15E-11
(OAO-2)		3.43E-09	2.33E-09	1.92E-09	1.37E-09	37699 B5 V	1.49E-10	6.16E-11	4.94E-11	5.45E-11
36541 B6 V	4.22E-09	3.86E-11	1.99E-11	2.66E-11	2.25E-11	37700 B5 V	2.61E-11	1.40E-11	1.38E-11	1.87E-11
36560 A0	7.93E-11	3.68E-11	2.13E-11	1.82E-11	1.30E-11	37742 O9.5 Ib	2.08E-08	9.93E-09	1.32E-08	1.65E-08
(TD-1)		3.68E-11	2.13E-11	1.82E-11	1.30E-11	(TD-1)	2.31E-08	9.93E-09	1.32E-08	1.65E-08
36591 B1 V	8.42E-10	7.13E-10	4.24E-10	4.30E-10	3.55E-10	37744 B1 V	1.94E-08	1.49E-08	1.43E-08	1.18E-08
(TD-1)		7.98E-10	6.03E-10	5.11E-10	3.84E-10	(OAO-2)	3.32E-08	2.69E-08	1.70E-08	1.28E-08
36629 B2 V	9.29E-11	5.94E-11	3.34E-11	3.05E-11	2.57E-11	37744 B1 V	5.06E-10	3.44E-10	2.36E-10	1.97E-10
36646 B3 V	1.34E-10	1.30E-10	7.07E-11	7.40E-11	7.07E-11	(TD-1)	8.78E-10	3.47E-10	2.17E-10	1.63E-10
36695 B1 V	7.92E-10	7.60E-10	5.66E-10	4.25E-10	4.78E-10	37756 B2 IV	9.62E-10	6.47E-10	5.78E-10	4.79E-10
(OAO-2)		1.11E-09	9.08E-10	6.70E-10	3.88E-10	(TD-1)	8.71E-10	7.88E-10	6.26E-10	4.79E-10
36779 B2 V	3.37E-10	2.14E-10	1.59E-10	1.43E-10	1.17E-10	37775 B2 V	2.22E-10	1.56E-10	8.73E-11	7.93E-11
(TD-1)		2.50E-10	1.89E-10	1.57E-10	1.17E-10	37807 B8	9.11E-11	5.95E-11	2.80E-11	2.47E-11
36827 B5	1.91E-10	1.32E-10	8.72E-11	9.13E-11	7.25E-11	37889 B2 V	7.17E-11	4.68E-11	3.62E-11	2.84E-11
(TD-1)		1.34E-10	1.09E-10	8.82E-11	6.85E-11					

NOTE.—The flux data from the TD-1 and OAO 2 experiments are given next to those from S520-3 whenever available, integrated to match with the passband.
* The flux data of HD 37041 (θ^1 Ori) include the fluxes of θ^1 Ori and its nebulosity.

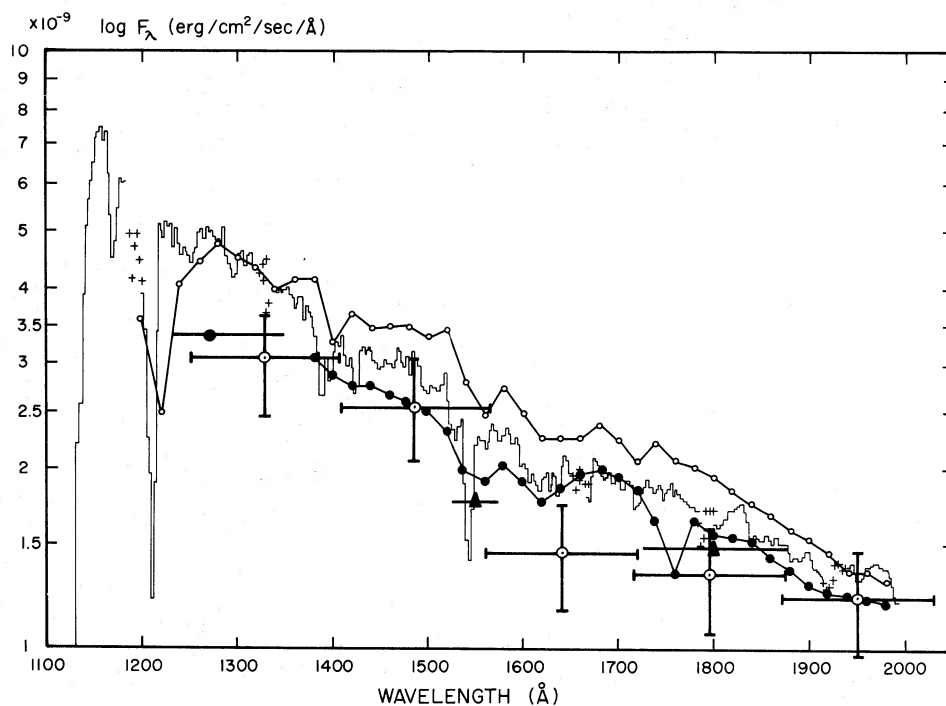


FIG. 3.—Observed flux distributions of ν Ori, (S520-3; dot-circles with error bars and passband ranges). Previous observations by satellites (OAO 2, open circles; TD-1, filled circles; IUE, histograms; ANS, triangles) and by rocket (Carruthers 1969; larger filled circle with passband range) are also plotted.

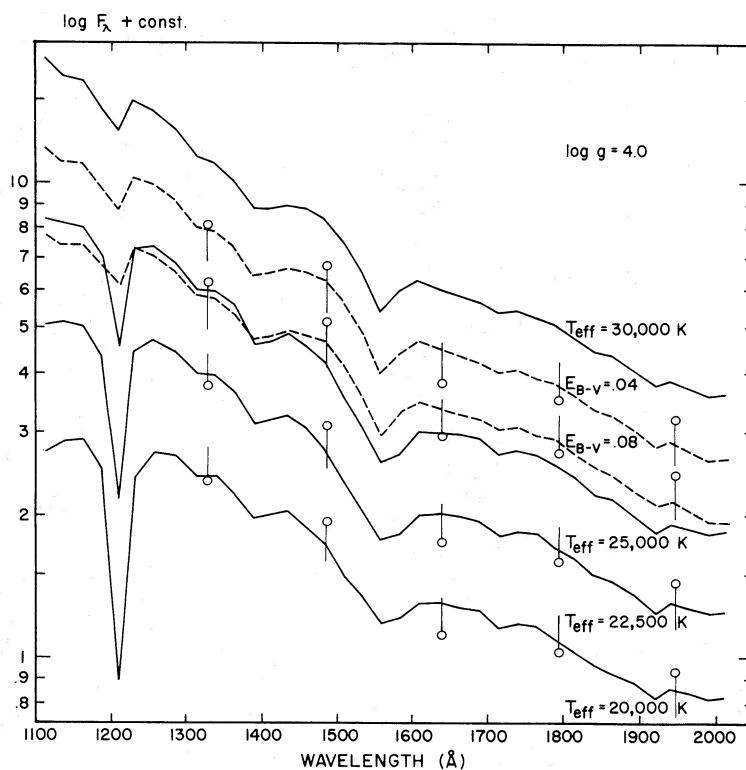


FIG. 4.—Comparison of the flux distribution of ν Ori between the observation and models. Kurucz models of $\log g = 4.0$ are shown for $T_{\text{eff}} = 30,000$ K [$E(B-V) = 0.00$, and by broken curves 0.04, 0.08], 25,000 K, 22,500 K, and 20,000 K. Fittings of our data are indicated by open circles with error bars of appropriate directions; see the text.

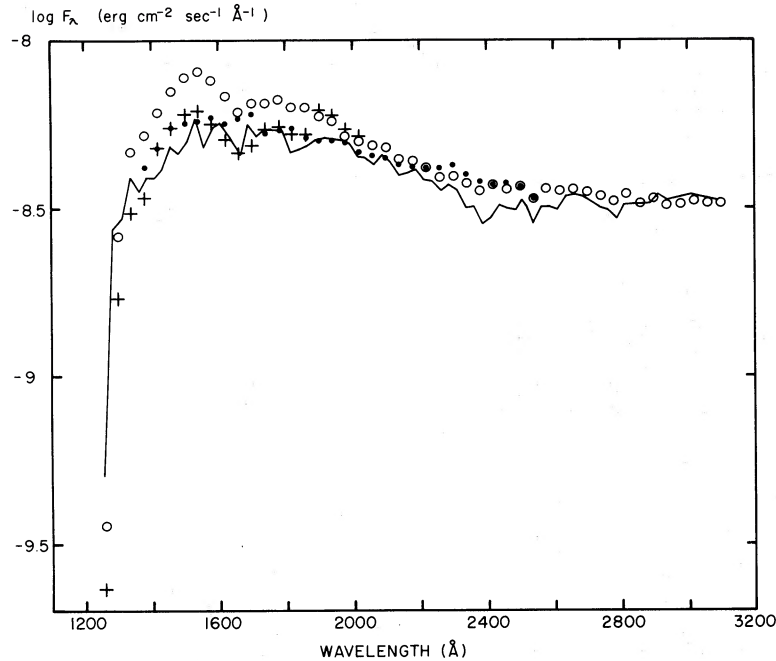


FIG. 5.—Flux distribution of α Lyr observed by OAO 2 (open circles) and TD-1 (dots). Corrected flux distribution of OAO 2 fluxes using our correction factors is indicated by pluses. Within one passband of our observation, fluxes are uniformly corrected. Flux distribution of Kurucz models having $T_{\text{eff}} = 9,400$ K ($\log g = 3.95$) are also indicated by lines.

The -10% correction around 1640 Å increases the amount of the excess flux in the model predictions for late-A type stars (Böhm-Vitense 1981; Crivellari and Praderie 1982), and the absorption edge of Si I 1680 Å appears more clearly in the corrected spectra. The treatment of line opacities around this wavelength should be reexamined in model calculations.

The new calibration may necessitate revisions of the energy distributions of extragalactic active objects with nonthermal emissions (quasars and BL Lac objects) (cf. Wilson, Carnochan, and Gondhalekar 1979; Snijders *et al.* 1979; Ulrich *et al.* 1980; Kondo *et al.* 1981). The suppression of the flux below 1500 Å substantially enlarges the spectral index α , when an approximated form of $f_\nu \propto \nu^{-\alpha}$ is assumed in the far-ultraviolet. In the case of BL Lac object, PKS 2155–304, simultaneously observed by IUE and Einstein (Urry *et al.* 1982), the increase of spectral index leads to a smooth extension of the UV flux level to the X-ray level. It may be worthwhile to reexamine the parameters in a synchrotron-Compton emission model for the ultraviolet and X-ray region, using the new calibration.

Isophote maps of the diffuse background radiation were produced after the subtraction of discrete sources and the background levels outside the Orion region. Figure 6 shows the spectral surface brightness integrated over annular zones between 1° and 4° radii centered at $\alpha = 5^{\text{h}}34^{\text{m}}$ and $\delta = -3^\circ$ (1950.0) within our observation field. This point is regarded to be the center of the general enhancement of the diffuse ultraviolet background in the Orion region (Carruthers and Opal 1977a, b). The error bars correspond to statistical errors. The large error bar for the 1328 Å channel, however, includes the uncertainty due to the suspected contamination by airglow (O I 1304 Å) of which only the maximum range could be very roughly estimated from the time and altitude variations of the background level. In Figure 6 the data from TD-1 (Morgan,

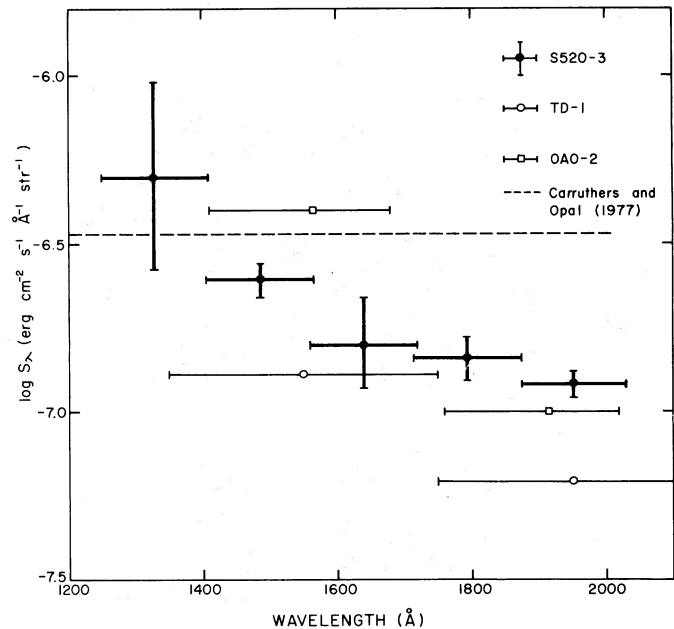


FIG. 6.—The spectral distribution of the diffuse background surface brightness in the Orion region. The integrated brightnesses between the radial distances $r = 1^\circ$ and 4° centered at $\alpha = 5^{\text{h}}34^{\text{m}}$ and $\delta = 3^\circ$ (1950.0) are indicated by filled circles with error bars. For comparison, the data from TD-1 (Morgan *et al.* 1982) and those from OAO 2 (Witt and Lillie 1978) are plotted by open circles and open squares, respectively. The average surface brightness of the Orion reflection nebulosity measured by Carruthers and Opal (1977a) is also shown by a dashed line.

Nandy, and Thompson 1982) and those from *OAO 2* (Witt and Lillie 1978) are also included. For the latter the integrated surface brightnesses between 1° and 4° were obtained from their fitted curves in a form of $S \propto r^{-P}$. The previous measurements with low spectral resolutions may be regarded to be compatible with the present data, although the error estimates are not explicitly published for the former. The present result clearly indicates a systematic increase of the diffuse ultraviolet flux toward shorter wavelengths. This trend coincides with the increase of the average extinction in the far-ultraviolet (Savage

and Mathis 1979) and suggests the higher albedo of interstellar grains in this wavelength range. This provides important information about responsible grain material in the far-ultraviolet region (cf. Huffman 1977) and will be discussed in detail in a forthcoming paper (Onaka *et al.* 1983).

The authors are deeply indebted to the ISAS staffs for their technical supports during the rocket experiments, and to Messrs. A. Yamaguchi, M. Nakagiri, K. Akita, T. Sasaki, and T. Tsujimura for their assistance in the laboratory work.

REFERENCES

- Beekmans, F. 1977, *Astr. Ap.*, **60**, 1.
 Blanco, V. M., Demers, S., Douglass, G. G., and FitzGerald, M. P. 1968, *Pub. US Naval Obs.*, **21**, 2d ser.
 Böhm-Vitense, E. 1981, *Ann. Rev. Astr. Ap.*, **19**, 295.
 Bohlin, R. C., Holm, A. V., Savage, B. D., Sniijders, M. A. J., and Sparks, W. M. 1980, *Astr. Ap.*, **85**, 1.
 Brune, W. H., Mount, G. H., and Feldman, P. D. 1979, *Ap. J.*, **227**, 884.
 Carruthers, G. R. 1969, *Ap. Space Sci.*, **5**, 387.
 Carruthers, G. R., Heckathorn, H. M., and Opal, C. B. 1981, *Ap. J.*, **243**, 855.
 Carruthers, G. R., and Opal, C. B. 1977a, *Ap. J. (Letters)*, **212**, L27.
 ———, 1977b, *Ap. J.*, **217**, 95.
 Code, A. D., and Meade, M. R. 1979, *Ap. J. Suppl.*, **39**, 195.
 Crivellari, L., and Praderie, F. 1982, *Astr. Ap.*, **107**, 75.
 Dreiling, L. A., and Bell, R. A. 1980, *Ap. J.*, **241**, 736.
 FitzGerald, M. P. 1970, *Astr. Ap.*, **4**, 1234.
 Henry, R. C., Weinstein, A., Feldman, P. D., Fastie, W. G., and Moos, H. W. 1975, *Ap. J.*, **201**, 613.
 Huffman, D. R. 1977, *Adv. Phys.*, **26**, 129.
 Hunter, W. R. 1974, *J. Spectr. Soc. Japan*, **23**, No. 1, 37.
 Jamar, C., Macau-Hercot, D., Monfils, A., Thomson, G. I., Houziaux, L., and Wilson, R. 1976, *Ultraviolet Bright-Star Spectrophotometric Catalogue* (ESA SR-27).
 Kondo, Y., *et al.* 1981, *Ap. J.*, **243**, 690.
 Kurucz, R. L. 1979, *Ap. J. Suppl.*, **40**, 1.
 Macau-Hercot, D., Jamar, C., Monfils, A., Thompson, G. I., Houziaux, L., and Wilson, R. 1978, *Supplement to the Ultraviolet Bright-Star Spectrophotometric Catalogue* (ESA SR-28).
 Meyer, D. M., and Savage, B. D. 1981, *Ap. J.*, **248**, 545.
 Morgan, D. H., Nandy, K., and Thompson, G. I. 1982, *M.N.R.A.S.*, **199**, 399.
 Nishi, K., Higashi, K., and Yamaguchi, A. 1970, *Tokyo Astr. Obs. Rept.*, **15**, 253 (in Japanese).
 Nishi, K., and Suemoto, Z. 1971, in *IAU Symposium 41, New Techniques in Space Astronomy*, ed. F. Labuhn and R. Lüst (Dordrecht: Reidel), p. 393.
 Onaka, T., Sawamura, M., Tanaka, W., Watanabe, T., and Kodaira, K. 1983, in preparation.
 Opal, C. B., Moos, H. W., Fastie, W. G., Bottema, M., and Henry, R. C. 1968, *Ap. J. (Letters)*, **153**, L179.
 Savage, B. D., and Mathis, J. S. 1979, *Ann. Rev. Astr. Ap.*, **17**, 73.
 Sniijders, M. A. J., Bokseberg, A., Barr, P., Sanford, P. W., Ives, J. C., and Penston, M. V. 1979, *M.N.R.A.S.*, **189**, 873.
 Stecher, T. P. 1968, in *An Introduction to Space Science*, ed. W. N. Hess and G. D. Mead (2d ed.; New York: Gordon and Breach), p. 285.
 Stronglylis, G. J., and Bohlin, R. C. 1979, *Pub. A.S.P.*, **91**, 205.
 Ulrich, M. H., *et al.* 1980, *M.N.R.A.S.*, **192**, 561.
 Urry, M., Holt, S., Kondo, Y., Mushotzky, R. F., Hackney, K. R. H., and Hackney, R. L. 1982, in *Advances in Ultraviolet Astronomy: Four Years of IUE Research*, ed. Y. Kondo, J. M. Mead, and R. D. Chapman (NASA CP-2238), p. 177.
 Wesselius, P. R., van Duinen, R. J., Aadlers, J. W. G., and Kester, D. 1980, *Astr. Ap.*, **85**, 221.
 Wilson, R., Carnochan, D. J., and Gondhalekar, P. M. 1979, *Nature*, **277**, 457.
 Witt, A. N., and Lillie, C. F. 1978, *Ap. J.*, **222**, 909.

KEIICHI KODAIRA, KEIZO NISHI, and TETSUYA WATANABE: Tokyo Astronomical Observatory, Mitaka, Tokyo, PC 181 Japan

TAKASHI ONAKA, MINEO SAWAMURA, and WATARU TANAKA: Department of Astronomy, Faculty of Science, University of Tokyo, Bunkyo-ku, Tokyo, PC 113 Japan